FUSION-FISSION ANALYSIS OF VARIOUS NUCLEI WITH $A_{CN} \sim 40 - 150$ FORMED VIA IDENTICAL PROJECTILE AND TARGET COMBINATIONS

A Dissertation

Submitted in Partial Fulfillment of the Requirement for the Award of Degree of

Master of Science

In

Physics

Submitted By:

Manish Kumar

Roll No. 301904008

Under the supervision of:

Dr. Manoj K. Sharma

Professor

TIET Patiala

SCHOOL OF PHYSICS AND MATERIALS SCIENCE

THAPAR INSTITUTE OF ENGINEERING AND TECHNOLOGY, PATIALA

PUNJAB-147004

JULY-2021

Dedicated to My Parents

and

To all my friends

TIET, PATIALA

Certificate

I hereby certified that the dissertation entitled **"FUSION-FISSION ANALYSIS OF VARIOUS NUCLEI WITH $A_{CN} \sim 40 - 150$ FORMED VIA IDENTICAL PROJECTILE AND TARGET COMBINATIONS"** is being submitted by **Manish Kumar** (Roll No. 301904008) for the award of the degree of **Master of Science, Physics** in the School of Physics and Materials Science, **Thapar Institute of Engineering and Technology, Patiala** under the supervision of **Prof. Manoj K. Sharma**.

I further declare that No part of the work reported in this dissertation has been submitted and will not be submitted to any other institute or university for the award of any other degree.

Manish Kumar.

Dated: 29.07.2021

Manish Kumar
301904008

It is certified that the above statement made by the student is correct to the best of my knowledge and belief.

29.07.2021

Dr. Manoj K. Sharma
Professor,
School of Physics and Materials science,
Thapar Institute of Engineering and Technology,
Patiala-147004,
PUNJAB.

Acknowledgment

First of all I would like to acknowledge with a sense of gratitude to my supervisor **Prof. Manoj K. Sharma**, Professor, Thapar Institute of Engineering and Technology, Patiala for providing me the opportunity and valuable guidance. I am incredibly thankful to them for their humility to take me as their student and believing in me to undertake the problem I was given during this work.

I am also extremely thankful to **Prof. O. P. Pandey**, Head, School of Physics and Materials Science, TIET, Patiala for providing the possible research facilities in the department.

I am highly obliged to **Ms. Shivani Jain**, Research Scholar, School of Physics and Materials Science, TIET, Patiala for the valuable guidance and suggestions during various stages of this work. Despite having a busy schedule she was always available for discussions and timely guidance. I would also like to extend my deepest gratitude to my parents for their love and support throughout this work. My appreciation also goes to all of my friends for their encouragement and support all throughout this work.

Manish Kumar

Contents

List of Figures

List of Tables

Abstract

The main emphasis of this dissertation is to investigate the heavy-ion reaction dynamics by studying the formation and decay of various compound nuclear systems formed via mass-symmetric colliding nuclei. The study is done using the semiclassical approach in Skyrme energy density formalism (SEDF). The fusion cross-sections of mass-symmetric reactions is investigated using Wong model and its extended version (ℓ-summed Wong method). The subsequent decay dynamics of hot and rotating compound nuclei formed via symmetric reactions is investigated with the use of collective clusterisation approach (Dynamical cluster-decay model DCM). The dissertation is organized into three chapters, as briefly discussed below:

Chapter 1 begins with the general introduction of nuclear physics and a brief account of heavy-ion reactions in low energy region, laid on the formation of compound nuclear systems and subsequent decay mechanisms. Beside this, the relevant effect of deformation and orientation is discussed in this chapter.

Chapter 2 represents the brief methodology used in the present work. For studying the formation and disintegration of excited compound nucleus (CN), the nucleus-nucleus interaction potential is calculated using SEDF, details of which are described here. In this description, the Wong model along with its extended version are also explained in brief. To analyze decay properties such as decay cross-sections, DCM build on the Quantum mechanical fragmentation theory (QMFT) along with its relevant parameters, is also outlined in this chapter.

Chapter 3 consists of calculations and results. In this recent work, the nuclear potential is calculated using SEDF approach for the mass-symmetric reactions, i.e $(^{19}F+^{19}F), (^{24}Mg+^{24}Mg), (^{28}Si+^{28}Si), (^{46}Ti+^{46}Ti), (^{64}Ni+^{64}Ni)$ and $(^{74}Ge+^{74}Ge)$. Since the projectile-target of above mentioned reactions are deformed, so the cold and hot optimum cases have been introduced in the calculation of fusion cross-sections, across the Coulomb barrier energies, using Wong model and extended ℓ-summed Wong model. To explore the fission dynamics of excited CN formed from symmetric reactions, DCM is applied to calculate the cross-sections at common excitation energy $E^*_{CN} = 45$ MeV which corresponds to above barrier region.

Chapter 1

Literature Review

1.1 Introduction

A human mind is always curious about discovering various laws related to physical phenomenon around them. With the advancement in science and technology, now it becomes possible to explore the relevant aspects and understand them in a better way. In the search of many years it has been observed that, the universe surrounding us is a dynamic place consisting of intricate series of different matter, which is further made up of tiny particles called atoms. These atoms are further comprised of positively and negatively charged particles. The discovery of electron by British Physicist J. J. Thomson had led to an indication that the atom had some internal structure, which is related to the dense or core region of an atom. The dense region of atom which is named as nucleus is comprised of protons and neutrons, also called as nucleons of an atomic nucleus. The endless efforts by scientists have proved the existence of nucleus and its constituent particles/nucleons. As if the experiment of radioactivity in 1896 by A. H. Bacquerel was the biggest aspiration towards the understanding of nuclear structure and related properties. After the discovery of nucleus, the fundamental nature of matter has been extensively explored. These consistent efforts of numerous physicists have inspired us to understand the atomic attributes and their usage in the physical world. For the fundamental research in this field, different nuclear transmutation experiments done by famous scientists such as Rutherford, Cock-Croft, Walton, Curie and Juliet etc had prompted new ideas to understand the nuclear structure, nuclear properties and nuclear forces. Till now, various experimental and theoretical approaches have been proposed to understand the static and dynamic properties of atomic nucleus. Over the years, many models have been developed which are able to reproduce many features of nuclei. There are numerous limitations, which are addressed by using modified versions of earlier models or by adopting new models. Due to the occurence of different kind of nuclear reactions operating at wide range of energies, the evolution of nuclear physics presently includes its applications in many fields, such as nuclear power, nuclear medicine, nuclear weapons, agriculture, industrial sectors and many more. These diverse applications in the field of nuclear physics have put this subject in limelight since last over a century.

1.2 Heavy-ion Fusion reactions

In the collision of two nuclei, a nuclear reaction process takes place, in which the final product nuclides can be different from the reactants. The colliding nuclear partners may belong to different mass region of the periodic table. But the present work has constrained its discussion with heavy-ion nuclei (which have mass number $A \geq 4$ and atomic number $Z \geq 2$). This nuclear reaction process which may be classified as Nuclear fusion, Nuclear fission and evaporation residue etc, play a very prominent role in the production of new elements and ignite the possibility of extension of the nuclear periodic table. Nowadays these kind of nuclear reactions are used as a path in understanding the distinct aspects of colliding nuclei formed under various conditions. Two nuclei of similar or dissimilar kinds brought together in close proximity may fuse in to one another, if sufficient amount of energy is acquired by the projectile nucleus. In a close proximity region, the interaction among two nuclei is associated with the repulsive and attractive forces, which shall be discussed later. On other hand, in the nuclear fission process the amalgamated nucleus stays for a very short life time in its excitation state (compound nucleus) and decays into two comparable fragments. On the other hand, a compound nucleus may also decay via very asymmetric fragments, where the light fragment is lighter than an alpha particle. Such process is termed as evaporation residue (ER). In present work, I have explored the fusion process and subsequent decay into fission or ER channel.

The nuclear reactions can be classified into three categories on the basis of energy acquired by incident projectile. These different regions are given as - (a) low energy region (E $<$ 15 MeV/nucleon), (b) intermediate energy region (15 $<$ E $<$ 500 MeV/ nucleon) and (c) the high energy region E $>$ 500 MeV/nucleon. Out of these categories, the heavy-ion induced reactions at the low energy range are of attention for the formation of compound nuclear system and subsequent decay stages. In heavy-ion induced reactions, the positively charged bare nuclei show repulsion due to long-range Coulomb force, however the short-range nuclear force raises attraction in the proximity region. Basically, the competition between these forces defines a potential barrier. Classically at below barrier energies the fusion is forbidden but quantum mechanically there is finite probability due to tunneling effect. The interacting nuclei may undergo fusion by overcoming

this Coulomb barrier or by tunneling through this barrier. In other words, the colliding particles should have sufficient kinetic energy to cross-over or tunnel across the Coulomb barrier.

Depending upon incident energy, angular momentum and mass of colliding nuclei, the interaction between two nuclei may lead to the composition of a compound nucleus (CN). The formation of such excited nucleus depends on various properties of incoming channel and has proved to be extremely successful in exploring the nuclear behavior below and above the Coulomb barrier. Generally, a compound nucleus once formed forgets the history of its formation. The mode of disintegration of CN depends mainly on the incident energy of beam, angular momentum and parity of excited state composite system. This criteria is known as Bohr's independent hypothesis. The validity of such hypothesis was experimentally verified by S.N. Ghoshal [1] in 1950, where reaction cross-sections of almost same order of magnitude were observed for particular reaction products formed via different entrance channels.

Nowadays nuclear fusion/fission reactions are used as a tool to understand the distinct aspects of nuclear reactions formed under numerous physical conditions. In present work, the fusion of two identical nuclei and their decay mechanisms are studied to understand the nuclear structure and related nuclear properties. For this purpose, the collision of symmetric nuclei have been performed for which mass-asymmetry parameter $\eta_A = \frac{A_1 - A_2}{A_1 + A_2}$ = 0, here A_i(i = 1, 2) is the mass of projectile and target nucleus.

1.3 Decay dynamics of Compound nucleus (CN)

The compound nuclear reactions characterized by fusion of target and projectile nuclei proceed via different decay modes. A lot of work has been done towards the understanding of stability aspects of nuclear systems. The compound nucleus decay involves mainly three decay modes - (a) Evaporation-residue (ER) or light particles (LPs), (b) intermediate mass fragments (IMFs) and (c) heavy mass fragments (HMFs)/fission. As the compound system formed in exotic state (hot and unstable), so it decays to its ground state via particle emission or fission which depends on excited compound nucleus properties. In light mass compound systems say, $A_{CN} \sim 60 - 80$ the fission yield is minimal and light particle emission is accompanied by intermediate mass fragment

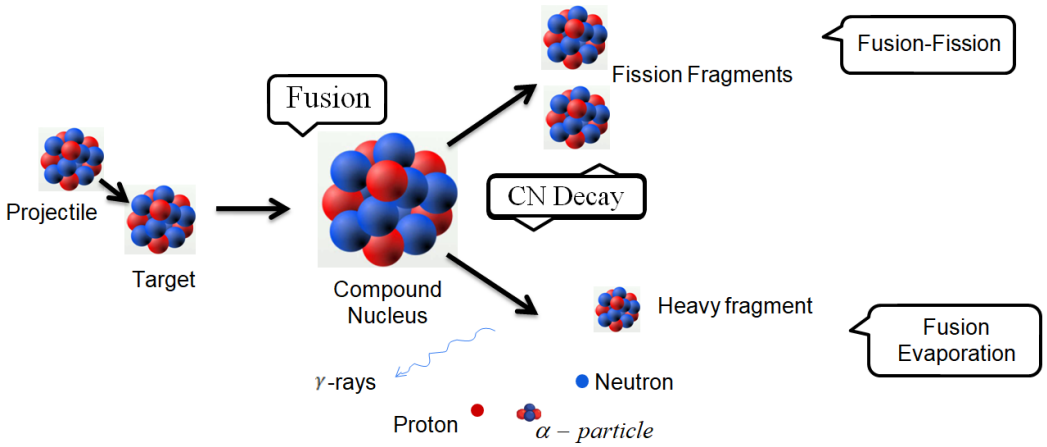

Figure 1.1: Schematic diagram for compound nucleus (CN) formation and subsequent decay mechanisms

(IMF), whose contribution may go upto $5-10\%$. In the intermediate compound systems $A_{CN} \sim 80-200$, there is competition between evaporation residue and fission due to enhancement in Coulomb repulsion. For heavier mass compound systems ($A_{CN} \sim 200$), the most probable decay mode is fission (either symmetric or asymmetric fission product) in which a compound nucleus splits into two fragments of comparable size, due to its instability against Coulomb repulsion. Therefore total fusion cross-section can be written as sum of fusion-evaporation and fission cross-sections. The schematic representation of different decay modes of compound nucleus formed is also shown in Fig. 1.1.

In recent times different statistical approaches were proposed to understand the decay dynamics of compound nucleus (CN) formed in various fusion reactions. The first such statistical hypothesis was developed by Bethe [2], Weisskopf [3] and Ewing [4]. In this method they explained the emission of neutrons and light charged particles, such as protons or $\alpha-particle$ from an excited state compound nucleus along with their emission probabilities at the low excitation energies. After that a quantum-mechanical approach by Hauser and Feshbach [5] has been proposed, where they calculated the cross-sections and emission probabilities between the discrete levels in terms of angular momentum. Proceeding this way, Bohr and Wheeler [6] suggested a theoretical approach to inspect nuclear fission process. After that different experimental and theoretical approaches were used to study the emission of intermediate mass fragments (IMFs) (which lies in the mass region $A_2 = 5-20$) and heavy mass fragments (HMFs) / fission (belong to $21 \leq A_2 \leq \frac{A_{CN}}{2} - 20$). To determine decay cross-sections many statistical codes like PACE [7],

CASCADE [8], (based on theory of Hauser and Feshbach) and BUSCO [9] were developed, which addressed the cross-sections through different routes.

Parallel to this, the Quantum Mechanical Fragmentation Theory (QMFT) [10, 11] was developed by Gupta and collaborators and is termed as Dynamical Cluster-decay model (DCM) [12]-[19]. This model have been established to study the heavy-ion reaction dynamics particularly for the decay of excited CN. This model is described in two phases: (i) the first phase describes the preformation of fragments (or clusters) in CN and (ii) in the next phase the preformed fragments begin to penetrate through the barrier. This model treats all the decay processes on the same footing. This model is a reformulation of PCM (preformed cluster model) in which collective-mass transfer phenomenon takes place. In the present work, the collective clusterization approach of this model has been applied to understand the decay mechanism and associated dynamical aspects. As the QMFT is developed on the fact that, the fragments/clusters are pre-born in the composite system. This quantum-mechanical preformation probability (P_o) of decaying fragments is calculated by obtaining the solution of Schrodinger equation. After the clusters formation their penetration probability across the interaction barrier can be calculated. The formalism of DCM based on QMFT is discussed in Chapter 2 along with its important parameters such as fragmentation potential (V_η), preformation probability (P_o) and penetration probability (P), which contributes to the decay cross-sections.

1.4 Nucleus-Nucleus interaction potential

The knowledge of nucleus-nucleus interaction potential is extremely desirable to study the heavy-ion induced fusion-fission reactions, as it is instrumental in fixing the barrier characteristics and associated nuclear phenomena such as fusion cross-sections. The ion-ion interaction potential is derived from the long-range repulsive and short-range nuclear attractive potentials. The repulsive potential comes into picture due to the positive charges of colliding partners, called as Coulomb potential and the rotational energy or (centrifugal potential) originated by angular momentum effect. On other hand, when two nuclei are separated with a very small distance of say < 2 fm, an attractive nuclear potential comes into consideration. The Coulomb and the angular-momentum interaction potentials are well described in the literature [20]. But the short-ranged nuclear interaction potential

depends upon the nuclear surface properties, and is relatively difficult to evaluate. Therefore different models have been developed by various authors to understand the complex behaviour of nuclear potential. It is relevant to note that an appropriate nuclear potential (ion-ion potential) is extremely desirable to address the governance of heavy-ion induced reactions. Many approaches have been used for the calculation of ion-ion interaction potential, for example in terms of effective two body interaction, and it is observed that effective nucleus-nucleus interactions can be worked out in terms of densities of colliding partners. Hence forth the energy density formalism (EDF) is used for the calculation of nucleus-nucleus interaction potential.

Utilization of semi-classical extended Thomas-Fermi approach (ETF) [21]-[24] within SEDF is extremely used to address heavy-ion induced reactions dynamics as it provides reasonable solutions in addressing the nucleus properties. The Hartree-Fock (HF) method, the microscopic background of the EDF model was given by Vautherin and Brink [25], investigate the ground-state properties of nuclei having spherical shapes with the use of Skyrme interactions [26]. Initially, the HF calculations did not include the kinetic energy density (τ) of the compound nucleus. To overcome this difficulty, the semi-classical approach based on Thomas-Fermi (TF) approach and its extension ETF has been employed.

The nuclear density is an important parameter used in calculation of ion-ion interaction potential within the SEDF approach. In literatures, different density functions have been used to extract appropriate barrier characteristics of the colliding nuclei. It has been observed in Ref. [27], that for the case of mass-symmetric reactions, the two-parameter nuclear density function (2pF) is enough for addressing the fusion cross-sections. The further details of this density distribution is explained in Chapter 2. From literature it is clear that, the utilization of different Skyrme forces give a range of fusion barrier characteristics, so numerous such combinations are explored (more than 300 parameter sets) [28], for appropriate addressal of nuclear properties. These parameters were fitted by different authors at different times and successfully used to reproduce various nuclear properties. In this work, the Skyrme force KDE0v1 [29] is used whose behavior is similar to that of SIII force, which is often used to study the heavy-ion induced reactions [30]-[31].

1.5 Deformation and orientation effects

There are numerous factors on which formation and disintegration of compound nuclear systems depends for example - mass, charge, angular momentum, deformations and orientations etc. Here, I concentrate on deformation and orientation degree of freedom, which is of foremost importance towards the understanding of nuclear reactions. The heavy-ion induced reactions are affected by the shape/structure of the colliding/decaying nuclei. The availability of different optical instruments till now, could not provide the facility to see any nucleus. But also some of observations and analyzed properties, extract the information about the shape, structure and orientation of nucleus. If a nucleus is identical in all aspects and in all dimensions, then we will see no change on its rotation. On other hand if a nucleus is deformed (non-spherical), we can see some changes on its rotation, which are its rotational characteristics. These observations convey the idea about distribution of nucleons inside the nucleus which leads to deformation degree of freedom. The interacting nuclei may have different shapes which is a measure of deviation from their spherical shape such as $\beta_{\lambda=2}, \beta_{\lambda=3}, \beta_{\lambda=4}$ which are quadrupole, octupole and hexadecupole deformations respectively. Among these deformations the quadruopole deformation (β_2) is most commonly observed shape, in which $\beta_2 < 0$ are called oblate and $\beta_2 > 0$ are called prolate. Both the shapes have symmetry around the axial and reflection axes. The contribution of the quadrupole deformation and orientation effects is very important in the formation of compound nucleus and its subsequent decay mechanisms. The elongated configuration of quadrupole deformed nuclei in reference to the colliding partners gives the largest interaction distance, which in turn lead to the lowest barrier heights. This process defines the cold synthesis of new element in fusion-fission process. On the other hand, the compact configuration of a deformed nucleus shows the smallest interaction distance and highest barrier height. This process is termed as the hot synthesis of approach. A detailed study has been given for quadrupole deformed nuclei in [32]-[34] that the cold and hot fusion phenomenon are explained on the basis of optimum orientations which depends on signs $(+/-)$ of quadrupole deformation. To observe the possible effect of deformation and orientations within the framework of Wong model, the calculations are done for different mass symmetric reactions and the results are compared with the experimental data, which is given around the Coulomb-barrier energies. These static

deformations are taken from reference [35]. Due to inclusion of deformations and orientations, the associated barrier characteristics (i.e. barrier height and barrier position) get affected and correspondingly influence the fusion-fission cross-sections.

1.6 Proposed Work

In the present work, the intention is to give a study for the fusion-fission dynamics of excited compound nucleus (CN), formed via mass-symmetric reactions, $(^{19}F+^{19}F), (^{24}Mg+^{24}Mg), (^{28}Si+^{28}Si), (^{46}Ti+^{46}Ti), (^{64}Ni+^{64}Ni)$ and $(^{74}Ge+^{74}Ge)$. For this analysis, the two-parameter Fermi (2pF) density function is used within the SEDF approach and studied the corresponding effects on barrier characteristics (i.e. barrier height and barrier position) and the fusion cross-sections. Since, the colliding nuclear partners of above mentioned reactions are quadrupole deformed (β_2), so the corresponding effects have been analyzed for the 'cold or elongated' and 'hot or compact' fusion configurations in the calculation of fusion cross-sectional area across the Coulomb barrier energies. At last, using the collective clusterization approach, the subsequent decay dynamics of compound nuclei (CN) formed using choosen set of symmetric reactions is analysed in the vicinity of Coulomb barrier.

Bibliography

[1] S. N. Ghoshal, Phys. Rev C **80**, 939 (1950).

[2] H. A. Bethe, Phys. Rev. **50**, 332 (1936); Rev. Mod. Phys. **9**, 69 (1937).

[3] V. WeissKopf, Phys. Rev. **52**, 295 (1937).

[4] V. WeissKopf and D. H. Ewing, Phys. Rev. **57**, 472 (1940).

[5] W. Hauser and H. Feshbach, Phys. Rev. **87**, 366 (1952).

[6] N. Bohr and J. A. Wheeler, Phys. Rev. **56**, 426 (1939).

[7] A. Gavron, Phys. Rev. C **21**, 230 (1980).

[8] F. Puhlhofer, Nucl. Phys. A **280**, 267-284 (1977).

[9] J. Gomez del Campo, *et al*, Phys. Rev. Lett. **61**, 290 (1988).

[10] J. Maruhn and W. Greiner, Z. Phys. **251**, 431 (1972); R. K. Gupta, W. Scheid and W. Greiner, Phys. Rev. Letts. **35**, 353 (1975).

[11] R. K. Gupta, *et al*, Phys. Rev. C **56**, 3242 (1997); R. K. Gupta, *et al*, J. Phys. G: Nucl. Part. Phys. **25**, L47 (1999); M. K. Sharma, R. K. Gupta and W. Scheid, J. Phys. G: Nucl. Part. Phys. **26**, L45 (2000).

[12] R. K. Gupta, edited by W. Greiner and R. K. Gupta, Heavy Elements and Related New Phenomenon, Vol.II, World Scientific, Singapore, p. 536, (Chapter14) (1999).

[13] R. K. Gupta, *et al*, J. Phys. G: Nucl. Part. Phys. **31**, 631 (2005); R. K. Gupta, M. Manhas and W. Greiner, Phys. Rev. C **73**, 054307 (2006).

[14] R. K. Gupta, in Cluster in Nuclei, Lecture Notes in Physics 818, Vol. I, edited by C. Beck (Springer-Verlag, Berlin), p. 223, (2010).

[15] G. Kaur and M. K. Sharma, Nucl. Phys. A **884**, 36 (2012); G. Kaur, *et al*, Nucl. Phys. A **927**, 232 (2014).

[16] G. Sawhney, *et al*, Phys. Rev. C **88**, 034603 (2013).

[17] N. Grover, *et al*, Nucl. Phys. A **959**, 10-26 (2017).

[18] M. Singh Gautam, N. Grover and M. K. Sharma, Eur. Phys. J. A **53**: 12 (2017).

[19] N. Grover, K. Sandhu and Manoj K. Sharma, Nucl. Phys. A **974**, 56-71 (2018).

[20] C. Y. Wong, Phys. Rev. Lett. **31**, 766 (1973).

[21] B. Grammoticos and A. Voros, Ann. Phys. **123**, 359 (1979).

[22] M. Brack, C. Guet and H. B. Hakansson, Phys. Rep. **123**, 275 (1985).

[23] B. Grammoticos and A. Voros, Ann. Phys. **129**, 153 (1980).

[24] J. Bartel and K. Bencheikh, Eur. Phys. J. A. **14**, 179 (2002).

[25] D. Vautherin and D. M. Brink, Phys. Rev. C **5**, 626 (1972).

[26] T. H. R. Skyrme, Phil. Mag. **1**, 1043 (1956); Nucl. Phys. **9**, 615 (1959).

[27] S. Jain, M. K. Sharma and R. Kumar, Nucl. Phys. A **997**, 121699 (2020).

[28] M. Dutra, *et al*, Phys. Rev. C **85**, 035201 (2012).

[29] B. K. Agrawal, S. Shlomo and V. K. Au, Phys. Rev. C **72**, 014310 (2005).

[30] O. N. Ghodsi and F. Torabi, Phys. Rev. C **92**, 064612 (2015).

[31] A. Deep *et al*, Int. J Mod. Phys. E Vol. 28, No. **10**, 1950079 (2019).

[32] R. K. Gupta, *et al*, J. Phys. G: Nucl. Part. Phys. C **31**, 631 (2005).

[33] K. Hagino, Phys. Rev. C **98**, 014607 (2018).

[34] G. Kaur, K. Sandhu and M. K. Sharma, Nucl. Phys. A **971**, 95-112 (2018).

[35] P. Moller, *et al*, At. Data and Nucl. Data Tables **109-110**, 1-204 (2016).

Chapter 2

Methodology

2.1 Introduction

Numerous theoretical efforts have been made to empathise the heavy-ion reaction mechanisms. Out of which, the explicit phenomenon of fusion-fission governed via disintegration of excited state compound nucleus is mostly studied mechanism towards the understanding of heavy-ion reaction dynamics. In this context, various theoretical models have been used with vital specifications. Proceeding that way, in the present work the process of formation of excited compound nucleus is studied using Wong model and its extended version (ℓ-summed Wong model) [1]-[4]. The penetration probability during the formation of such composite system is calculated using Hill-Wheeler approximation [5]. The decay mechanism is studied by employing the framework of Dynamical cluster decay model (DCM) [6]-[8]. To understand the formation and decay of composite systems, the systematic understanding of ion-ion interaction potential is necessary. For calculation of such nuclear interaction potential through the energy density formalism (EDF), the kinetic energy and relevant spin-orbit terms are obtained from extended Thomas-Fermi (ETF) approach, calculated using two-parameter Fermi (2pF) density function. The details are discussed in the subsequent sections. The Dynamical cluster decay model (DCM) is used to account the decay dynamics of compound nucleus which is formed from the heavy-ion induced reactions. This theory on which the model is based is Quantum mechanical fragmentation theory (QMFT). The details of Wong formula and its extended version (i.e. ℓ-summed Wong formula) which accounts all contributing ℓ-values, are used for estimation of fusion cross-sections are given in sections 2.3.1 and 2.3.2 respectively. The details of quantum-mechanical fragmentation theory (QMFT) are given in section 2.4, and DCM parameters such as fragmentation potential (V_η), preformation probability (P_o), penetration probability (P) and decay cross-sections are discussed in further sections 2.4.1, 2.4.2, 2.4.3 and 2.4.4 respectively.

2.2 Skyrme Energy Density Formalism (SEDF)

In the last few decades several methods have been developed for the calculation of ion-ion interaction potential. One of that kind of approach by Vautherin and Brink [9] is used in the present work, which uses a density dependent Skyrme interactions that

are parameterized in terms of two parameter-Fermi (2pF) density function. The main advantage of using this formalism is that it is capable of reproducing the various ground state properties of nuclear systems. Beside this one can segregate the spin-dependent and spin independent components of nuclear potential. The ion-ion interaction potential of two colliding nuclei is also known as total interaction potential expressed as, $V(R) = V_C(R) + V_N(R) + V_\ell(R)$. Using energy density formalism (EDF), the nucleus potential as a function of separation distance 'R' is calculated from the difference in the expectation values of energies obtained for nuclei separated at distance 'R' and at infinite distance, which is given as, $V_N(R) = E(R) - E(\infty)$.

The Skyrme Hamiltonian density $H(\vec{r})$ is then defined in relation to the expectation energy as,

$$E(R) = \int H(\vec{r}) d(\vec{r}) \tag{2.1}$$

where, Hamiltonian density $H(\vec{r})$ is a function of the nucleonic density (ρ), kinetic energy density (τ) and spin-orbit density ($\vec{J}$) and is reads as [9],

$$\begin{aligned}
H(\rho,\tau,\vec{J}) = {} & \frac{\hbar^2}{2m}\tau - \frac{1}{2}t_o\left[(x_o+\frac{1}{2})(\rho_n^2+\rho_p^2) - (1+\frac{1}{2}x_o)\rho^2\right] \\
& - \frac{1}{2}\sum_{i=1}^{3} t_{3i}\rho^{\alpha_i}\left[(x_{3i}+\frac{1}{2})(\rho_n^2+\rho_p^2) - (1+\frac{1}{2}x_{3i})\rho^2\right] \\
& + \frac{1}{4}\left[t_1(1+\frac{1}{2}x_1) + t_2(1+\frac{1}{2}x_2)\right]\rho\tau \\
& + \frac{1}{4}\left[t_2(x_2+\frac{1}{2}) - t_1(x_1+\frac{1}{2})\right](\rho_n\tau_n + \rho_p\tau_p) \\
& - \frac{1}{16}\left[t_2(1+\frac{1}{2}x_2) - 3t_1(1+\frac{1}{2}x_1)\right](\vec{\nabla}\rho)^2 \\
& - \frac{1}{16}\left[3t_1(x_1+\frac{1}{2}) + t_2(x_2+\frac{1}{2})\right] \\
& \times \left[(\nabla\rho_n)^2 + (\nabla\rho_p)^2\right] \\
& - \frac{1}{2}W_o\left[\rho\vec{\nabla}\cdot\vec{J} + \rho_n\vec{\nabla}\cdot\vec{J_n} + \rho_p\vec{\nabla}\cdot\vec{J_p}\right] \\
& - A\left[\frac{1}{16}(t_1x_1 + t_2x_2)\vec{J}^2\right] + A\left[\frac{1}{16}(t_1 - t_2)(\vec{J_p}^{\,2} + \vec{J_n}^{\,2})\right]
\end{aligned} \tag{2.2}$$

In semi-classical microscopic approach, the density approximations depending on time of collision between two ions are classified as sudden density approximation and frozen

density approximation. In present calculations frozen density approximation is used in which densities are added as $\rho = \rho_1 + \rho_2$, and for composite system kinetic energy and spin-orbit density terms are written as, $\tau(\rho) = \tau_1(\rho_1) + \tau_2(\rho_2)$ and $\vec{J}(\rho) = \vec{J_1}(\rho_1) + \vec{J_2}(\rho_2)$ respectively, with $\rho_i = \rho_{in} + \rho_{ip}, \tau_i(\rho_i) = \tau_{in}(\rho_{in}) + \tau_{ip}(\rho_{ip})$ and $\vec{J}_i(\rho_i) = \vec{J_{in}}(\rho_{in}) + \vec{J_{ip}}(\rho_{ip})$.

For the calculation of target-projectile density (ρ_i), the two-parameter Fermi (2pF) density function is used which reads as follows,

$$\rho_i(z_i) = \rho_{0i}\left[1 + \exp\left(\frac{z_i - R_{0i}}{a_i}\right)\right]^{-1}, -\infty \leq z \leq \infty. \tag{2.3}$$

where ρ_{0i} is the central density term calculated by solving the integral of nuclear density [10] and comes out as,

$$\rho_{0i} = \frac{3A_i}{4\pi R_{0i}^3}\left[1 + \frac{\pi^2 a_i^2}{R_{0i}^2}\right]^{-1} \tag{2.4}$$

Here R_{0i} is spherical half-density radius (in fm) and a_i is surface thickness (in fm), are known as 2pF density parameters. The polynomials of these parameters are obtained by fitting the data taken from [11].

Different Skyrme forces are used by different authors by fitting the various parameters. Out of different sets of parameters leading to different Skyrme forces, the force KDE0v1 is used in the present analysis whose behaviour is found to be similar to that of widely used Skyrme force SIII. The formation process of different mass-symmetric reactions are studied by Wong formula and its extended version (i.e. ℓ-summed Wong formula) and subsequent decay processes are analysed with the help of Dynamical cluster decay model (DCM) which are described in further sections.

2.3 Wong formula and Extended ℓ-summed Wong formula

2.3.1 Wong Formula

According to Wong [1] the fusion cross-sections for deformed nuclei having relative orientation angle (θ_i), which collide with incident energy i.e. $E_{c.m.}$ is given by,

$$\sigma(E_{c.m.}, \theta_i) = \frac{\pi}{k^2}\sum_{\ell=0}^{\ell_{max}}(2\ell+1)P_\ell(E_{c.m.}, \theta_i), \tag{2.5}$$

Here, $k = \sqrt{\frac{2\mu E_{c.m.}}{\hbar^2}}$, '$\mu$' is reduced mass and '$P_\ell$' is the transmission coefficient for each ℓ-values.

For assimilating the shape of ℓ-dependent interaction barrier $V_\ell(R, E_{c.m.}, \theta_i)$ through an inverted harmonic oscillator, Hill-Wheeler approximation is used and penetrability P_ℓ in terms of its barrier characteristics is given by,

$$P_\ell = \frac{1}{\left[1 + exp\left(\frac{2\pi(V_B^\ell(E_{c.m.},\theta_i) - E_{c.m.}}{\hbar\omega_\ell(E_{c.m.},\theta_i)}\right)\right]} \tag{2.6}$$

Here the curvature $\hbar\omega_\ell$ is obtained at barrier position 'R_B', which is in corresponding to the maximum barrier height at 'V_B', reads as

$$\hbar\omega_\ell(E_{c.m.}, \theta_i) = \hbar\left[\frac{|d^2V^\ell(R)/dR^2|_{R=R_B^\ell}}{\mu}\right]^{1/2}, \tag{2.7}$$

and barrier position R_B^ℓ is calculated using, $|dV_T^\ell(R)/dR|_{R=R_B^\ell} = 0$

2.3.2 Extended ℓ-summed Wong formula

The calculation of barrier position (R_B^ℓ) and curvature ($\hbar\omega_\ell$) using Eq. (2.7) justify that these quantities are insensitive to ℓ-values. In 2009, Gupta and collaborators [3] carried out ℓ-summation in equation (2.5) using ℓ_{max} determined empirically from best fit of measured cross-section, which is given as

$$\sigma_{fus}(E_{c.m.}, \theta_2) = \frac{\pi}{k^2}\sum_{\ell=0}^{\ell_{max}} \frac{(2\ell+1)}{\left[1 + \exp\left(\frac{2\pi}{\hbar\omega_B^\ell}(V_B^\ell - E_{c.m.})\right)\right]}. \tag{2.8}$$

2.4 Dynamical cluster-decay model (DCM)

The relative probability by which the compound nucleus may decay into different decay channels is explained on the basis of Dynamical cluster decay model (DCM). This model is originated from the Quantum mechanical fragmentation theory (QMFT), which describes the interaction among two bodies which are involved in nuclear fusion and fission processes. The QMFT uses the concept of quantum mechanical probability to explore different decay mechanisms.

To study variety of decay paths, DCM have been successfully applied and includes all the essential components, likewise excitation energy (E^*_{CN}), temperature (T), deformations ($\beta_{\lambda i}$) and orientations (θ_i), angular momentum (ℓ), etc. To study these decay processes, the mass asymmetry coordinate (η_A) is used to describe the exchange of nucleon (protons and neutrons) among decaying fragments and relative separation coordinate (R) describes the amount of kinetic/incident energy ($E_{c.m.}$) of incoming channel transferred to the outgoing channel (or emitting particles). The excitation energy (E^*_{CN}) is related to incident energy ($E_{c.m.}$) and temperature (T) by the following relation [12],

$$E^*_{CN} = E_{c.m.} + Q_{in} = \frac{1}{a}AT^2 - T. \tag{2.9}$$

In the above expression, 'a' is called as a level density parameter. In the present work, we are working for mass-range of compound nuclear systems A_{CN}=40-150. For light- to heavy-mass systems, the choice of a is 8 and 9, respectively.

2.4.1 Fragmentation Potential (V_η)

The fragmentation potential gives the structural information about the decaying nucleus and acts as an input parameter for the calculation of preformation probability (P_o) is given by,

$$\begin{aligned} V_\eta(R,T,\ell) &= V_C(R,T,Z_i,\beta_{\lambda i},\theta_i,\phi) + V_\ell(R,T,A_i,\beta_{\lambda i},\theta_i,\phi) \\ &\quad + V_N(R,T,A_i,\beta_{\lambda i},\theta_i,\phi) - \sum_{i=1}^{2} B_i(T,A_i,Z_i,\beta_{\lambda i}). \end{aligned} \tag{2.10}$$

Here, $B_i(i=1,2)$ are the binding energies of interacting nuclei, V_C and V_ℓ are Coulomb and angular momentum potentials which depends on temperature, deformations and orientations etc. The V_N is the attractive nuclear proximity potential, which is derived using SEDF approach (as discussed in earlier section).

2.4.2 Preformation Probability (P_o)

The preformation probability (P_0) is an essential parameter of DCM which gives an opportunity to analyze the mass division of decaying fragments and the solution of time-independent Schrodinger equation gives P_0, as given below

$$P_o = |\psi(\eta(A_i^2))|\sqrt{\beta_{\eta\eta}}\frac{2}{A_{CN}}. \tag{2.11}$$

In the above expression, the mass-parameter that is $\sqrt{\beta_{\eta\eta}}$ defines the kinetic energy [13], and A_{CN} is the mass of compound nucleus formed.

2.4.3 Penetration Probability (P)

The penetration probability or barrier tunneling probability of preformed fragments decaying from the excited compound nucleus is calculated using WKB approximation [14] and is given by relation,

$$P = exp\left[-\frac{2}{\hbar}\int_{R_a}^{R_b}\sqrt{2\mu[V(R)-Q_{eff}]}dR\right] \tag{2.12}$$

Here, $V(R)$ and Q_{eff} are the scattering potential and effective Q-value, respectively, of decay process. The limits in above integral indicate the penetration of fragment through the interaction barrier starting point (R_a) and terminating point (R_b).

2.4.4 Decay Cross-Sections

After obtaining preformation probability (P_o) and penetration probability (P), the compound nucleus (CN) decay cross-sections are calculated within decoupled approximations by applying partial wave analysis (PWA) as,

$$\sigma_{DCM} = \frac{\pi}{k^2}\sum_{\ell=\ell_{min}}^{\ell_{max}}(2\ell+1)P_oP; \tag{2.13}$$

Here, the relations of 'k' and 'μ' are already discussed in the above section. 'ℓ_{max}' is termed as the maximum value of angular momentum and m is nucleon mass. Here ℓ_{max} corresponds to value where the evaporation residue cross-section becomes zero i.e. $\sigma_{ER} \to 0$.

Using Eq. (2.13), the Evaporation Residue and fission cross-sections are studied as given

below,

$$\begin{aligned} \sigma_{ER} &= \sum_{A_2=1}^{4} \sigma(A_1, A_2); \\ \sigma_{ff} &= \sum_{A_2=\frac{A}{2}-20}^{A/2} \sigma(A_1, A_2) \end{aligned} \tag{2.14}$$

Using these cross-sections, the total cross-section of compound nucleus (CN) is obtained as $\sigma_{CN} = \sigma_{fusion} = \sigma_{ER} + \sigma_{ff}$.

Bibliography

[1] C. Y. Wong, Phys. Rev. Lett. **31**, 766 (1973).

[2] R. Kumar, *et al*, Phys. Rev. C **80**, 034618 (2009).

[3] R. Kumar, M. K. Sharma and R. K. Gupta, Nucl. Phys. A **870-871**, 42 (2011).

[4] D. Jain, *et al*, Phys. Rev. C **85**, 024615 (2012).

[5] D. L. Hill and J. A. Wheeler, Phys. Rev. **89**, 1102 (1953); T. D. Thomas, ibid. **116**, 703 (1959)

[6] R.K. Gupta, *et al*, Phys. Rev. C **71**, 014601 (2005).

[7] B. B. Singh, *et al*, Int. J. Mod. Phys. E **15**, 699 (2006).

[8] B. B. Singh, M. K. Sharma and R. K. Gupta, Phys. Rev. C **77**, 054613 (2008).

[9] D. Vautherin and D.M. Brink, Phys. Rev. C **5**, 626 (1972).

[10] L. R. B. Elton, Nuclear Sizes, Oxford University Press, London, (1961).

[11] L. R. B. Elton, Proc. Phys. Soc. Lond. A **63**, 1115 (1950).

[12] K. J. LeCouteur and D. W. Lang, Nucl. Phys. **13**, 32 (1959).

[13] H. Kroger and W. Scheid, J. Phys. G **6**, L85 (1980).

[14] G. Wentzel, Z. Phys. **38**, 518 (1926); H. A. Kramers, Z. Phys. **39**, 828 (1926); L. Brillouin, Compt. Rend. Hebd. Seances Acad. Sci. **183**, 24 (1926).

Chapter 3

Fusion-Fission analysis of various nuclei with $A_{CN} \sim 40 - 150$ formed via identical projectile and target combinations

3.1 Calculations and Results

The phenomena of formation and decay of excited compound nucleus (CN*) have been of huge interest, as one can understand various important aspects related to the reaction dynamics across the Coulomb barrier energies. Thus, the present chapter aims to study the formation and disintegration of various compound nuclei formed in the mass range of ($38 \leq A_{CN}{}^* \leq 148$) formed via various mass-symmetric ($\eta_A = \frac{|A_1-A_2|}{|A_1+A_2|}$=0) reactions, i.e. $^{19}F + ^{19}F$, $^{24}Mg + ^{24}Mg$, $^{28}Si + ^{28}Si$, $^{46}Ti + ^{46}Ti$, $^{64}Ni + ^{64}Ni$ and $^{74}Ge + ^{74}Ge$. To carried out this work, the Skyrme energy density formalism (SEDF) of Vautherin and Brink [1] has been considered for the calculation of nucleus-nucleus interaction potential. In the above calculations, the parameters of KDE0v1 Skyrme force are taken into account as described in earlier chapters. Note that, in the chosen set of reactions, the identical colliding particles are taken as prolate ($\beta_2 > 0$) as well as oblate ($\beta_2 < 0$) quadrupole deformed nuclei. In order to identify the comparative change in the barrier parameters (i.e. barrier height 'V_B', barrier position 'R_B' and barrier curvature '$\hbar\omega_B$') with the inclusion of β_2 - deformation and optimum (hot and cold) orientations effects, the total interaction potential V_T varies with the change in the separation distance R. Later, the collective impact of V_B, R_B and $\hbar\omega_B$ is worked out in the measurements of the fusion cross-sections, using the Wong's formula [2] and ℓ-summed Wong formula [3]. The outcomes obtained from Wong model are also compared with the experimental data, given across the Coulomb barrier energies, for the above mentioned reactions [4]-[9]. For the decay analysis, the dynamical cluster decay-model (DCM) [10]-[12] is employed to calculate the evaporation residue (ER) cross-sections at excitation energy (E^*_{CN}=45 MeV), which corresponds to the energy $E_{c.m.}$ (MeV) above the Coulomb-barrier. Additionally, the mass distribution of compound nuclei (i.e. ^{38}Ar, ^{48}Cr, ^{56}Ni, ^{92}Ru, ^{128}Ba and ^{148}Gd), formed via above mentioned mass-symmetric reactions, is illustrated to study the relative emergence of decaying fragments (A_1, A_2) in the fission region.

3.1.1 Barrier characteristics with the effect of $\beta_2^{\pm}$ and θ_{opt}

In order to understand the possibility of fusion among similar kinds of colliding nuclei, the fusion cross-section depending on the barrier is determined for a wide range of center of mass energy $E_{c.m.}$ (MeV). But, initially, the barrier parameters, which are barrier height

V_B, barrier position R_B and barrier curvature $\hbar\omega_B$, are derived from the total interaction potential, V_T(R). Important to note that, as a constituent and an essential term of V_T, the nuclear potential $V_N(R)$ is calculated by employing the parameters of KDE0v1 Skyrme force within the SEDF approach. As stated already, the target-projectile (of same mass) possess quadrupole (β_2) deformations with different signs (+/-). The nuclei $^{46}Ti(\beta_2 = 0.021)$, $^{19}F(\beta_2 = 0.262)$ and $^{24}Mg(\beta_{21} = 0.393)$ of the considered choices of nuclear reactions are of prolate shape (β_2^+), and $^{64}Ni(\beta_2 = -0.094)$, $^{74}Ge(\beta_2 = -0.237)$ and $^{28}Si(\beta_2 = -0.363)$ are of oblate shape (β_2^-) with magnitude of quadrupole deformation parameter. In view of this, the total potential $V_T(R)$ is plotted for reactions involving colliding partners of prolate shape β_2^+ and related optimum orientations (θ_{opt}) defining the 'hot or compact' and 'cold or elongated' fusion configurations, see panels (a)-(c) of Fig.3.1. The results are also compared with the spherical configuration of colliding nuclei. So, one can clearly see that, as the magnitude of β_2^+ increases, a significant modification is seen on barrier height 'V_B' and corresponding position 'R_B' for both the cold and hot optimum cases.

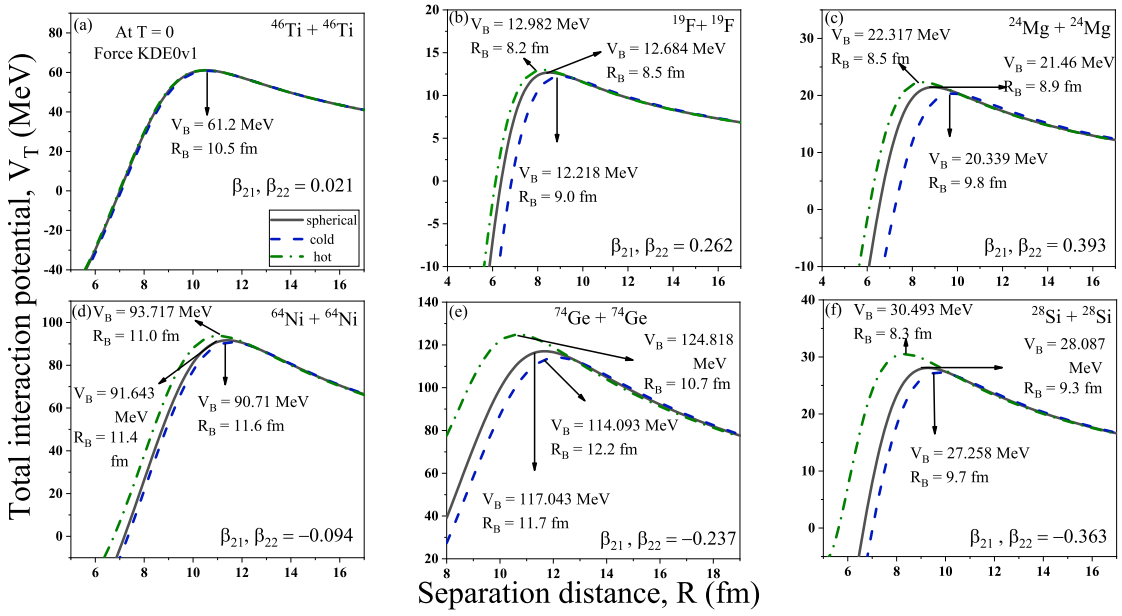

Figure 3.1: The behavior of total potential, V_T (MeV) is represented as a function of the separation distance, R (fm) for different choices of mass-symmetric reactions, which involve target-projectile of (a)-(c) prolate shape (β_2^+), and (d)-(f) oblate shape (β_2^-). The results obtained due to 'hot' (or compact) and 'cold' (or elongated) configurations of quadrupole deformed nuclei are also compared with that of the spherical configuration of considered reactions.

Similarly, in the lower panels (d)-(f) of Fig.3.1, the higher magnitude of oblate shape β_2^- of above mentioned nuclear reactions shows relatively stronger impact on V_B and R_B, in reference to that of spherical configuration. The changes observed in these barrier characteristics, with the effect of β_2 and θ_{opt} degrees of freedom, can be further analyzed in determining the fusion cross-sections (σ_{fus}), which are calculated using Wong's formula [2] and ℓ-summed formula [3]. The calculated cross-sections are compared with the data of the selected nuclear reactions, across the Coulomb barrier energies. The experimental measurements of fusion cross-sections for ^{19}F+^{19}F and ^{24}Mg+^{24}Mg reactions are given for above-barrier energies only. The fusion cross-sections of these reactions are predicted, in order to analyze the influence of β_2^+ along with θ_{opt} of hot and cold configurations of the shape, at the below and near-barrier energies.

3.1.2 Calculation of fusion cross-sections across the Coulomb barrier

For the calculation of fusion cross-sections (σ_{fus}) of various compound nuclei belonging to the mass-region $A_{CN}{}^* = 38$ - 148 formed via mass-symmetric ($\eta = 0$) reaction partners, the Wong's formula is employed. In Fig.3.2, the fusion cross-sections across the Coulomb barrier energies, for the selected choices of nuclear reactions, are compared with the available experimental data of $^{19}F + ^{19}F$, $^{24}Mg + ^{24}Mg$, $^{28}Si + ^{28}Si$, $^{46}Ti + ^{46}Ti$, $^{64}Ni + ^{64}Ni$ and $^{74}Ge + ^{74}Ge$ reactions [4]-[9]. The σ_{fus}(mb) obtained with the inclusion of β_2^+ along with θ_{opt} of cold and hot fusion configurations for $^{46}Ti + ^{46}Ti$, $^{19}F + ^{19}F$ and $^{24}Mg + ^{24}Mg$ reactions is shown in panels (a), (b) and (c) respectively of Fig.3.2. For below-barrier energies, σ_{fus} for both the cold and hot optimum cases give reasonably good agreement with the available data of $^{46}Ti + ^{46}Ti$ reaction, the cold configuration though seems to give relatively better agreement. As evident from Fig.3.1, there is a very nominal change in V_B and R_B for compact and elongated configurations, due to small magnitude of β_2^+ of ^{46}Ti. For $^{19}F + ^{19}F$ and $^{24}Mg + ^{24}Mg$ reactions, the below barrier data is not available in [4, 5]. So, I have calculated the fusion cross-sections at sub-barrier region for both the hot and cold optimum cases of these reactions. One may notice the modification in σ_{fus}, as we shift from the compact to elongated configuration of $^{19}F + ^{19}F$ and $^{24}Mg + ^{24}Mg$ nuclear partners, due to relatively larger magnitude of β_2^+. At above barrier region, both compact and elongated configurations seem to address the available data, particularly for the cases with higher magnitude of β_2^+.

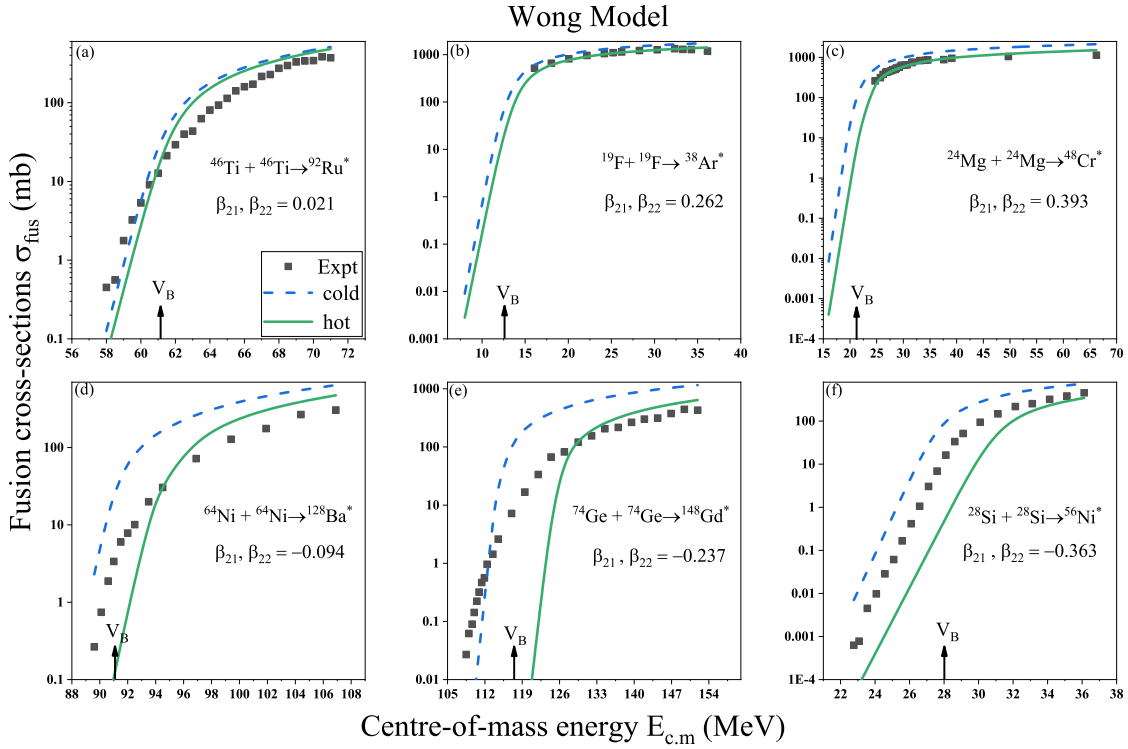

Figure 3.2: The fusion cross-sectional area σ_{fus}(mb) calculated using Wong formula for reactions involving β_2^+, i.e. (a) $^{46}Ti + ^{46}Ti$, (b) $^{19}F + ^{19}F$ and (c) $^{24}Mg + ^{24}Mg$, and β_2^- in (d) $^{64}Ni + ^{64}Ni$, (e) $^{74}Ge + ^{74}Ge$ and (f) $^{28}Si + ^{28}Si$. Also, the experimental data of above mentioned reactions [4]-[9] is shown for comparison.

Later, the fusion cross-sections are calculated for reactions, which involve oblate (β_2^-) deformed target-projectile nuclei, i.e. $^{28}Si + ^{28}Si$, $^{64}Ni + ^{64}Ni$ and $^{74}Ge + ^{74}Ge$. In this case, one can notice that, the elongated or cold configuration of oblate shape nuclei overestimates the experimental data across the Coulomb barrier energies for the above mentioned reactions, except for $^{74}Ge + ^{74}Ge$, see panels (d)-(f) of Fig.3.2. On the other hand, for compact or hot configuration of oblate deformed colliding partners, significant fusion hinderance is observed. It is important to mention that, for $^{74}Ge + ^{74}Ge$ reaction at deep sub-barrier region, the hindrance observed is relatively less for cold configuration of β_2^- than that of hot configuration. Overall, one can say that at below barrier energies, the elongated configuration of either prolate or oblate shape nuclei involved in mass-symmetric reactions give relatively better results, as compared to the compact configuration of quadrupole deformed nuclei.

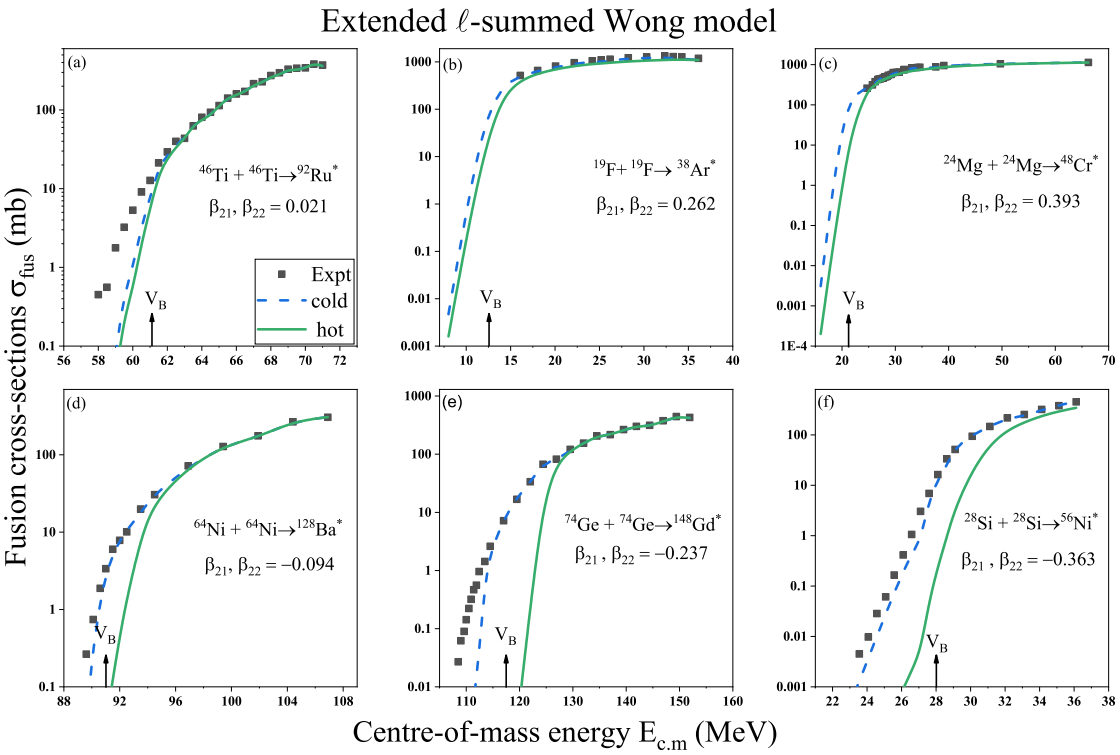

Figure 3.3: Same as Fig.3.2, but σ_{fus}(mb) obtained using extended ℓ-summed Wong model. Using sharp cut-off model [13], the ℓ-values are determined for above barrier energies and extended for below ones.

In the Wong formula [2], the fusion cross-sections are calculated or summed up for infinite ℓ-values. So, σ_{fus} determined for some reactions overestimate the data over a wide range of incident energies. In order to overcome from this issue, Gupta and his collaborators have made an explicit summation of ℓ-values under some approximations and elaborated an extended version of Wong model, or extended ℓ-summed Wong model [3]. In the present work, the Sharp cut-off model [13] is used to calculate ℓ_{max}-values for above barrier energies. These values are extended for sub-barrier region. Therefore, for a reaction, the ℓ-values are same whether including θ_{opt} of cold or hot fusion configurations of $\beta_2^{\pm}$ nuclei. In Fig.3.3, the calculation of fusion cross-sections from ℓ-summed model are depicted for the considered choices of mass-symmetric reactions, with respect to the incident energy $E_{c.m.}$(MeV).

From Figs. 3.2 and 3.3, one can conclude that, the elongated configuration of either prolate or oblate shapes with larger magnitude of β_2-deformation addresses the data for below- as well as above-barrier energies. On the other hand, the hot configuration gives good agreement with the available data only for the above barrier energies. In addition to the above, the decay analysis of excited compound nuclei (CN*), formed via considered

choices of symmetric reactions, has been studied with the use of dynamical cluster-decay model (DCM). The results of decay dynamics are discussed in the next section.

3.1.3 Decay analysis of excited CN* formed via symmetric reactions at $E^*_{CN} = 45MeV$

In the present work, to study the decay dynamics, the symmetric reactions ($\eta_A = 0$) are chosen where the target and projectile nuclei have same mass and charge number. In the above discussion, the signature of quadrupole deformation and optimum orientations (related to the cold and hot fusion configurations) has been explored at the below- as well as above-barrier energies. The 'cold or elongated' configuration addresses the data for the below barrier energies using ℓ-summed model. On the other hand, for above-barrier energies, the 'hot or compact' configuration gives similar results as that of cold optimum case and reproduces the experimental data of considered choices of symmetric reactions. The experimental measurements of cross-sections for $^{19}F + ^{19}F$, $^{24}Mg + ^{24}Mg$, $^{28}Si + ^{28}Si$, $^{46}Ti + ^{46}Ti$, $^{64}Ni + ^{64}Ni$ and $^{74}Ge + ^{74}Ge$ nuclear partners are related to the fusion/evaporation-residue (ER) process. So, in the present work, the ER cross-sections are also calculated using the DCM model, with the incorporation of quadrupole and hot optimum orientation of the emitting nuclei.

In DCM model, the neck-length parameter '$\triangle R$' has permissible value upto 2 fm and known as a single parameter. To examine the variation of $\triangle R$, the ER cross-sections are calculated for different compound nuclei formed via symmetric reactions, at a common excitation energy $E^*_{CN} = 45$ MeV which corresponds to the above-barrier incident energy $E_{c.m.}$, see Table 3.1. In this table, the ER cross-sections calculated using DCM are found near to the experimental data, at a fixed value of $\triangle R$. One can see from the table that, the evaporation residual cross-sections for light-mass compound nuclei (i.e. A_{CN}=38, 48 and 56) is comparatively larger than that of heavy-mass CN (A_{CN}=92, 128 and 148). This motivates us to analyze the contribution of fission process in the decay of light to heavy-mass compound nuclei, formed from considered choices of symmetric reactions.

Table 3.1: The ER cross-sections with relevant variables calculated using DCM for selected choices of symmetric reactions, at a common excitation energy E^*_{CN}=45 MeV. The calculated values are compared with the available data [4]-[9].

Reaction	$E_{c.m}$ (MeV)	T (MeV)	ΔR_{ER} (fm)	ℓ_{max} ($\hbar$)	σ_{ER} Expt. (mb)	σ_{ER} DCM (mb)
^{19}F+^{19}F$\rightarrow^{38}$Ar*	14.24	3.185	1.052	27	167.9	166.0
^{24}Mg+^{24}Mg$\rightarrow^{48}$Cr*	27.83	2.823	1.50	28	466.0	464.6
^{28}Si+^{28}Si$\rightarrow^{56}$Ni*	30.32	2.771	1.255	29	94.27	94.7
^{46}Ti+^{46}Ti$\rightarrow^{92}$Ru*	60.47	2.148	1.0	44	9.06	9.99
^{64}Ni+^{64}Ni$\rightarrow^{128}$Ba*	93.63	1.814	1.325	63	19.9	19.87
^{74}Ge+^{74}Ge$\rightarrow^{148}$Gd*	116.40	1.685	1.25	77	7.18	7.11

It is known from literature [14] that, the ER process is comparatively a fast process, in reference to the fission. This aspect may be correlated through the neck-length parameter, by adopting relatively higher neck length parameter for ER process as compared to that for the fusion. On the basis of this fact, the fission possibility has been analyzed in terms of the mass-distribution/preformation probability P_0 of excited CN* of mass-region $A_{CN} = 38 - 148$. The preformation probability P_0 gives the structure of preformed clusters formed inside the compound nucleus, the results are shown in Fig.3.4. From panels (a)-(c) of this figure, one can see for light-mass compound nuclear systems (^{38}Ar*, ^{48}Cr* and ^{56}Ni*) that, the most probable decaying fragments (A_1, A_2) belong to intermediate-mass fragments (IMF) region i.e. A_2=5-20. In the fission region, the value of P_0 is relatively smaller for the above mentioned light-mass CN. On the other hand, in panel (d) of Fig.3.4, the fission component starts competing with the IMF region, for ^{92}Ru* case. The panels (e) and (f) represent the symmetric mass-distribution of the decaying fragments in fission region of ^{128}Ba* and ^{148}Gd* compound nuclear systems. In other words, as one moves from light-mass compound nuclear system to heavy-mass, the

mass-distribution gets transferred from asymmetric to symmetric region.

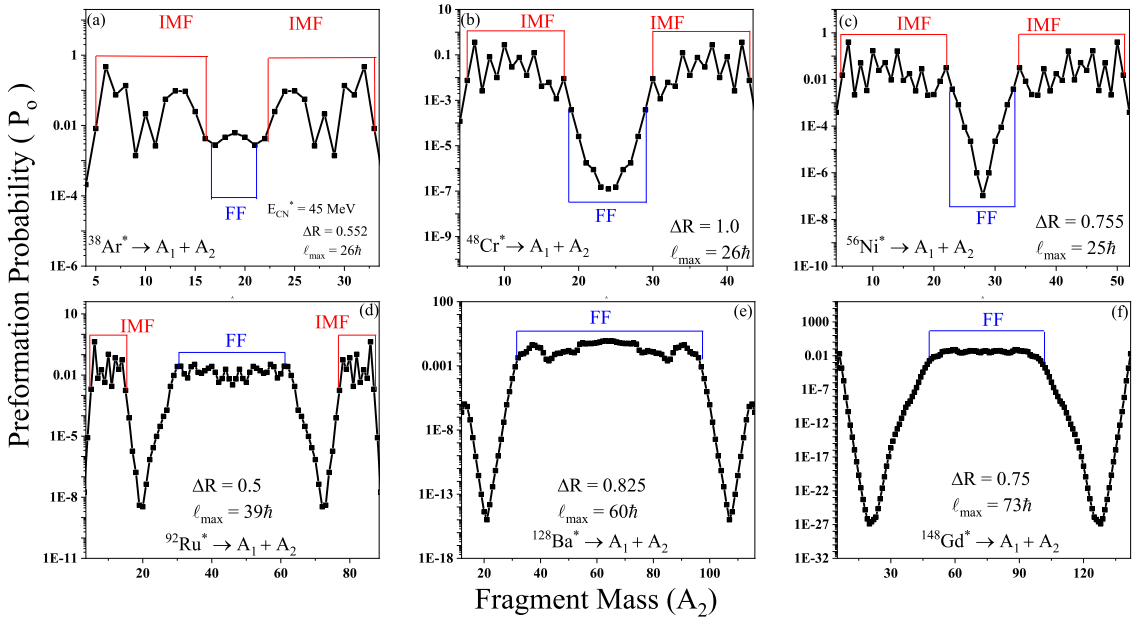

Figure 3.4: Comparison of Preformation probability P_0 for the decay of various compound nuclei, formed from (a) $^{19}F + ^{19}F$, (b) $^{24}Mg + ^{24}Mg$, (c) $^{28}Si + ^{28}Si$, (d) $^{46}Ti + ^{46}Ti$, (e) $^{64}Ni + ^{64}Ni$ and (f) $^{74}Ge + ^{74}Ge$ reactions, is shown with respect to fragment mass A_2.

From above results and discussion, it would be interesting to explore the variation of neck-length parameter for a large variety of compound nuclei, formed from mass-symmetric and asymmetric reactions, for the above- as well as below-barrier energies. Additionally, for these nuclear systems, the behavior of mass and charge distributions can be analyzed in our future work.

Summary

In the present work, the role of quadrupole deformation and optimum orientations (related to the compact and elongated fusion configurations) has been investigated in view of formation and decay channel of nuclear reactions involving identical projectile and target nuclei, i.e. $^{19}F + ^{19}F$, $^{24}Mg + ^{24}Mg$, $^{28}Si + ^{28}Si$, $^{46}Ti + ^{46}Ti$, $^{64}Ni + ^{64}Ni$ and $^{74}Ge + ^{74}Ge$ reactions. Firstly, the calculation of fusion cross-sections is done with the use of Wong model and the overestimation of cross-section at above barrier region is resolved by employing ℓ-summed Wong model. The β_2-deformed elongated configuration seem to provide relatively better option, particularly at sub-barrier region. However, the compact configuration of $\beta_2^{\pm}$ hinders the fusion among identical kinds of colliding nuclei at below barrier, and gives agreement with the data only at above barrier energies.

Afterwards, the evaporation residual (ER) cross-sections have been calculated using the collective clusterization approach of DCM for various excited compound nuclei, formed via considered choices of symmetric reactions, at a common excitation energy E^*_{CN} which corresponds to the above-barrier region. For lighter-mass CN (^{38}Ar*, ^{48}Cr* and ^{56}Ni*), the ER cross-sections are much higher, as compared to heavy-mass region, i.e. ^{92}Ru*, ^{128}Ba* and ^{148}Gd*. Consequently the possibility of fission component is explored for heavier nuclei. The preformation probability P_0 of fission fragments comes out to be higher for the heavier compound nuclear systems. In other words, intermediate mass fragments (IMFs) are more prominent than fission fragments for the light mass compound nuclear systems.

Future Scope: In the future work, one can consider a large variety of compound nuclear systems, formed via mass-symmetric ($\eta_A = 0$) and asymmetric ($\eta_A \neq 0$) nuclear reactions, to study the fusion-fission dynamics. Also, the octupole and hexadecapole deformations along with appropriate orientation degree of freedom may employed to extract explicit role of deformations in symmetric and asymmetric nuclear reactions.

Bibliography

[1] D. Vautherin and D. M. Brink, Phys. Rev. C **5**, 626 (1972).

[2] C. Y. Wong, Phys. Lett. B **31**, 766 (1973).

[3] R. Kumar, *et al*, Phys. Rev. C **80**, 034618 (2009).

[4] R. M. Anjos, *et al*, Phys. Rev. C **42**, 354 (1990).

[5] C. M. Jachcinski, *et al*, Phys. Rev. C **24**, 2070 (1981).

[6] G. Montagnoli, *et al*, Phys. Rev. C **90**, 44608 (2014).

[7] A. M. Stefanini, *et al*, Phys. Rev. C **65**, 34609 (2002).

[8] M. Beckerman, *et al*, Phys. Rev. C **25**, 837 (1982).

[9] M. Beckerman, *et al*, Phys. Rev. C **28**, 1963 (1983).

[10] R. K. Gupta, *et al*, Phys. Rev. C **71**, 014601 (2005).

[11] B. B. Singh, *et al*, Int. J. Mod. Phys. E **15**, 699 (2006).

[12] B. B. Singh, M. K. Sharma and R. K. Gupta, Phys. Rev. C **77**, 054613 (2008).

[13] M. Beckerman, *et al*, Phys. Rev. C **23**, 4 (1981).

[14] M. Kaur and M. K. Sharma, Eur. Phys. J. A **50**, 61 (2014).